Int. J. Environ. Sci. Technol. (2016) 13:2001–2010
DOI 10.1007/s13762-016-0989-0

ORIGINAL PAPER

# Experimental study of pure and mixtures of $CO_2$ and $CH_4$ adsorption on modified carbon nanotubes

**E. Molyanyan[1] · S. Aghamiri[1] · M. R. Talaie[1] · N. Iraji[1]**

Received: 2 March 2015 / Revised: 8 February 2016 / Accepted: 12 April 2016 / Published online: 28 April 2016


**Abstract** In this work 3-[2-(2-aminoethylamino)ethylamino]propyl trimethoxysilane (TRI) was employed to functionalize MWCNT containing hydroxyl groups (OH-MWCNT), and the XRD, FTIR, TGA and CHNS elemental analysis techniques were used to characterize the resulted adsorbents. The characterization results for amine-MWCNT showed amine groups effectively attached to the surface of the MWCNT. The equilibrium adsorption capacity of pure $CO_2$ and $CH_4$ and their binary mixture on the pristine MWCNT, OH-MWCNT and amine-MWCNT was measured through a set of equilibrium adsorption experiments at 303.2 and 318.2 K. Capacities of all three types of adsorbents for $CO_2$ adsorption were higher than those for methane adsorption. Also, amine-MWCNT demonstrated better performance on $CO_2$ adsorption than the other two adsorbents, especially at low partial pressures. The capacity of amine-MWCNT for pure $CO_2$ adsorption was 2.5 and 4 times as much as those for pristine MWCNT and OH-MWCNT, respectively, at the temperature of 303.2 K and the pressure of 0.2 bar. The binary adsorption experiment revealed that $CO_2/CH_4$ selectivity for pristine MWCNT and amine-MWCNT in all molar fractions of $CO_2$ is about 1.77 and 7, respectively.

**Keywords** Adsorption · Carbon dioxide · Carbon nanotube · Functionalization · Methane · Natural gas

✉ S. Aghamiri
aghamiri@eng.ui.ac.ir

[1] Department of Chemical Engineering, Faculty of Engineering, University of Isfahan, P.O. Box 81746-73441, Isfahan, Iran

## Introduction

There are some irrefutable proofs in the literature that reveal major global warming has been initiated due to releasing greenhouse gases to the atmosphere (Fatemi et al. 2011; Sayari et al. 2011; Zhang et al. 2010b). Global warming triggers dangerous changes in the earth's climate and environment (Lithoxoos et al. 2010; Plaza et al. 2007). The primary concern is the emission of carbon dioxide and methane that have been harmfully increased by anthropogenic activities (Ottiger et al. 2008). Approximately, 30 % of carbon dioxide emission is associated with fossil-fuel combustion (Sayari et al. 2011), while the methane emission mainly stems from agricultural activities (Ottiger et al. 2008). Methane is also produced through the anaerobic biodegradation of organic pollutants (Zamora et al. 2010). Separation of carbon dioxide from natural gas creates the beneficial effect of increasing natural gas heating value in addition to reducing greenhouse gas emissions (Fatemi et al. 2011; Tagliabue et al. 2011).

Different technologies may be employed to remove, capture or separate $CO_2$ from a mixture of gases including absorption, adsorption, cryogenics and membranes (Hsu et al. 2010; Zhao et al. 2010). $CO_2$ adsorption on solid adsorbents is carried out for different purposes such as removing $CO_2$ from flue gas or natural gas (Xiao et al. 2008; Zhang et al. 2010a) and sequestering $CO_2$ by burial of the adsorbents filled by $CO_2$ (Su et al. 2009). Adsorption is usually employed to facilitate the transportation or storage of methane as well (Vela and Huarte-Larrañaga 2011). Methane can be stored in the form of adsorbed natural gas (ANG) at relatively low pressure and ambient temperature. It is more advantageous than liquefied natural gas (LNG) and compressed natural gas (CNG) which require high pressure and low temperature (Dai et al. 2008).

Separation and sequestration of greenhouse gases have been performed using porous adsorbents such as activated carbons (Labus et al. 2014), coal (Zhang et al. 2014), zeolites (Deng et al. 2012; Pham et al. 2014; Silva et al. 2014), metal–organic frameworks (MOFs) (Saha et al. 2010), single-walled carbon nanotubes (SWCNTs) (Lithoxoos et al. 2010; Mahdavifar and Haghbayan 2012) and MWCNTs (Fatemi et al. 2011; Su et al. 2009). The appropriate sorbent should possess a several properties including good chemical and thermal stability, high adsorption capacity and selectivity, fast kinetics, convenient regeneration and low cost (Lithoxoos et al. 2010; Sayari et al. 2011). In recent decades, application of carbon nanotubes (CNTs) in many areas has been developed due to their unique structure, inestimable mechanical and thermal properties, excellent electrical conductivity and porous nature (Oriňáková and Oriňák 2011; Wiśniewski et al. 2012). Since the outer layer of CNT is inert and hydrophobic, their applications are restricted (Chiang et al. 2012; Ju et al. 2010). On the other hand, the large adsorption capacity of carbon nanotube relies upon its pore structure and presence of functional groups on their surface (Su et al. 2009). Functionalization is an effective method to improve CNT's dispersion into water and increase adsorption capacity (Vuković et al. 2009, 2010). CNTs can be functionalized in the forms of either covalent or noncovalent (Balasubramanian and Burghard 2005; Kuzmany et al. 2004; Sinnott 2002). The functionalization process can be performed through either single-step or two-step procedures. In the two-step process, after oxidizing pristine CNTs, they are modified by amidation or esterification reactions, while, in the single-step method, functional groups are attached directly to the sidewalls of pristine CNTs (Vuković et al. 2009, 2010). Oxidation of CNTs has been extensively investigated (Chiang and Wu 2010; Trykowski et al. 2010; Xu et al. 2011). Amino functional groups have a high tendency to combine with other functional groups and form more complex structures. The formation of amino groups on CNTs improves their catalytic activity and alkaline level and hence increases their capacity and selectivity for the adsorption of the acidic gases such as $CO_2$ and $SO_2$ (Fatemi et al. 2011). Lithoxoos et al. (2010) performed both experimental and theoretical investigation on the adsorption of pure $CH_4$, $N_2$, CO and $CO_2$ gases on oxidized MWCNTs. They found that the capacity magnitude followed the order of $H_2 \ll N_2 \approx CH_4 < CO \ll CO_2$. Vela and Huarte-Larrañaga (2011) studied the adsorption of methane in CNT through determining the influence of the nanotube diameter on the adsorption capacity by employing molecular dynamics (MD) simulation. They found out that the adsorption capacity was raised as nanotube diameter increased. Nickmand et al. (2013) used Grand Canonical Monte Carlo (GCMC) simulation to model adsorption of $CO_2$ and $SO_2$ molecules by pristine and functionalized SWCNTs. Their results showed that the adsorption capacity for $SO_2$ was generally higher than that for $CO_2$, especially at low pressures. Su et al. (2009) reported a set of experiments conducted for the adsorption of $CO_2$ on MWCNT containing amine groups. They found that the MWCNT modified by 3-aminopropyl-triethoxysilane (APTS) solution showed higher adsorption capacity than the pristine ones. Gholami et al. (2014) functionalized both bimodal-porous and pore-expanded MCM-41 samples utilizing TRI solution. They compared the amine-grafting performance and $CO_2$ adsorption capacities of both samples. Their results showed that the adsorption capacity of the pore-expanded samples was higher than that of the bimodal-porous ones. In addition, they concluded that the void volume of the adsorbent was a key factor in influencing the adsorption capacity of the amine-grafted adsorbents. Fatemi et al. (2011) produced nitrogenated MWCNTs (N-MWCNTs) through the reaction of ammonia with oxygenated MWCNTs (O-MWCNTs). They also investigated the adsorption capacity and selectivity of $CO_2$ and $CH_4$ on N-MWCNTs. According to their results, N-MWCNTs demonstrated higher capacity and selectivity to adsorb $CO_2$ than O-MWCNTs did. Zhang et al. (2010a) studied adsorption behavior of $CO_2/CH_4$ mixture on SWCNTs and MCM-41 using Grand Canonical Monte Carlo (GCMC) simulations. According to the results, the selectivity of MCM-41 for separation of $CO_2/CH_4$ was insensitive to the bulk mole fraction, whereas the selectivity of SWCNT changes significantly with bulk mole fraction. Huang et al. (2007) performed Grand Canonical Monte Carlo (GCMC) simulations to study the adsorption of $CO_2/CH_4$ mixture and the effect of temperature, pressure and pore size in carbon nanotubes. They found that the CNTs have a preferential adsorption of $CO_2$ in the binary $CO_2/CH_4$ mixture. The results show that for CNTs with diameter less than 1.1 nm, temperature and pressure have little effect on adsorption behavior and selectivity, whereas for the large CNTs, temperature and pressure have significant effects.

This work is devoted to evaluate methods for modification of the MWCNT-based adsorbent for $CO_2$ adsorption in order to separate $CO_2$ from $CH_4$. In this work, two types of O-MWCNTs, hydroxylated MWCNT (OH-MWCNT) and carboxylated MWCNT (COOH-MWCNT), are employed to produce amine-functionalized MWCVT utilizing TRI solution by two slightly different methods. The adsorption capacity of modified adsorbents will be used to select functionalization method. Also, the capacity and selectivity of adsorbents will be measured at temperatures of 303.2 and 318.2 K and pressures up to 3 bar by employing the static volumetric method.

## Materials and methods

MWCNT, COOH-MWCNT and OH-MWCNT were purchased from Neunano Company and used as received. Specifications of MWCNT, COOH-MWCNT and OH-MWCNT are shown in Table 1. TRI was purchased from Sigma-Aldrich. Toluene and n-hexane were purchased from Merck Company. High-purity grade $CO_2$ and $CH_4$ with the purity of 99.995 % were purchased from Farafan Gas Company and Technical Gas Services, respectively.

### Functionalization of MWCNTs

The COOH-MWCNT and OH-MWCNT were functionalized using TRI solution employing the following procedure (Harlick and Sayari 2007; Gholami et al. 2014): X-MWCNT (X denotes both COOH and OH) was dehydrated at 393.2 K for 2 h in an oven. Then, it was dispersed into a flask containing 75 ml of toluene. The mixture was stirred using magnetic stirrer for 3 h at room temperature. Then, the temperature was increased to 358 K, and TRI (1.5 ml) was added to the mixture followed by refluxing for 16 h. The produced solution was filtered, and the filtered solid was washed with toluene and *n*-hexane. Finally, the solid product was dried at 353 K in an oven for 2 h. These final products were labeled as COOH-amine-MWCNT and OH-amine-MWCNT, respectively. The above-mentioned method was applied on OH-MWCNT with slight changes, as follows: The OH-MWCNT was dehydrated at 393.2 K for 2 h in oven. Then, it was dispersed into a flask containing 75 ml of toluene. The mixture was stirred using magnetic stirrer for 30 min at room temperature. Next, 0.3 ml of water was added to the mixture. After 10 min of sonication, mixture was stirred for more 3 h. Later on, the temperature was increased to 358 K, and 1.5 ml TRI was added to the mixture followed by refluxing for 16 h. The mixture was filtered and washed with toluene and n-hexane. Finally, the filtered solid was dried at 353 K in an oven for 2 h. This final product was labeled as amine-MWCNT. The difference between these two methods is referred to use water during functionalization in the latter.

### Characterization of MWCNTs

The adsorbents were characterized by Fourier transform infrared spectroscopy (FTIR), X-ray diffraction (XRD), thermal gravimetric analysis (TGA) and elemental analysis (CHNS). FTIR spectra were recorded on a Fourier transform infrared spectrophotometer [JASCO, FT/IR-6300 (400–4000 $cm^{-1}$), Japan]. The last was used to perform a qualitative analysis of the functional groups. Thermal analysis was carried out in a thermogravimetric analyzer (Rheometric Scientific) at a heating rate of 10 °C/min. CHNS analysis was obtained by elemental analyzer (LECO Co., 932) which was employed to determine the chemical composition of adsorbents and evaluation of amine content on A-WCNT. XRD data were obtained using an X-ray diffractometer (Bruker, D8 Advance, Germany, wavelength: 1.7890 °A (Co Kα), voltage: 40 kV, current: 40 mA), in order to determine the structure of adsorbents.

### Apparatus and procedure

#### *Single-component gas adsorption*

The equilibrium adsorption experiments were carried out in a volumetric setup. This setup contained two cells. Gas was entered the first cell, known as loading cell, from a storage cylinder and was permitted to flow to the second cell, known as adsorption cell, through a needle valve. The volume of loading and adsorption cells was 75.2755 and 27.9752 ml, respectively. The pressure in each cell was measured by a pressure transducer (M5156-11700X-070BG, Sensys Co., Korea) with an uncertainty of ±1 kPa.

**Table 1** Specification and structural properties of MWCNT, COOH-MWCNT and OH-MWCNT

| CNTs[a] | MWCNT | OH-MWCNT | COOH-MWCNT |
|---|---|---|---|
| Outer diameter (nm) | <8 | <8 | <8 |
| Inner diameter (nm) | 2–5 | 2–5 | 2–5 |
| Length (μm) | >10 | 10–30 | 10–30 |
| Special surface area ($m^2$/g) | >500 | >500 | >500 |
| Electric conductivity (s/cm) | >100 | >100 | >100 |
| Purity (%) | >95 | >95 | >95 |
| –OH content (wt%) | – | 5.58 | – |
| –COOH content (wt%) | – | – | 3.86 |

[a] Raw multi-walled carbon nanotube (RAW-MWCNT), hydroxylated MWCNT (OH-MWCNT) and carboxylated MWCNT (COOH-MWCNT)

Temperatures were controlled on both cells by a circulating system (Arian Azma Co., Iran) and measured by PT100 thermocouple with ±0.1 K accuracy.

In the adsorption cell, 0.5 g ± 0.1 mg of the adsorbent after eliminating the impurity traces at 453.2 K is placed. Then, loading cell is filled by either $CO_2$ or $CH_4$ up to a desired pressure and its temperature is adjusted at the predetermined values using circulating system. Next, the gas in the loading cell is transferred to the adsorption cell up to a desired pressure, while temperature is regulated by using a circulating system. The adsorption equilibrium state is detected when the pressure of adsorption cell maintains at a constant value.

*Adsorption of binary mixtures*

To measure equilibrium of $CO_2$–$CH_4$ adsorption on adsorbents, a simple but robust closed-loop volumetric apparatus was employed (Fig. 1). The system consists of two cells (loading and adsorption cell), a variable-speed circulating pump, a pressure transmitter and an RTD temperature sensor. To measure the equilibrium adsorption data of $CO_2$–$CH_4$, first the adsorbent was degased and after eliminating the impurity traces at 100 °C are placed in the adsorption cell. It should be noticed that before loading the adsorbent the whole volume of the setup was purged by $N_2$. During loading the adsorbent and purging by $N_2$, the valves 4, 5, 8 and 9 were open and the rest were closed. After loading, the valve 4 was closed and pressure was increased to 1-bar gauge. Then, the valves 5 and 9 were closed and the loading cell was filled by definite molar percentage of $CH_4$ and $CO_2$ with total pressure the same as the pressure of adsorption cell. After preparing the adsorbing gas in loading cell, the valves 5 and 9 were opened and the circulating pump was turned on. Due to the adsorption of gas, the pressure changed, and the amount of the total adsorbed gas was calculated based on the total pressure change after enough time. In order to measure molar percentage of $CH_4$ and $CO_2$ in final gas, the composition was analyzed with a gas chromatograph (GC Agilent Technologies, N6890).

The selectivity of $CO_2$ over $CH_4$ in binary mixtures is determined using the following equation:

$$S_{CO_2/CH_4} = \frac{x_{CO_2}/x_{CH_4}}{y_{CO_2}/y_{CH_4}} \quad (1)$$

where $x$ and $y$ refer to the molar composition of the adsorbed phase and the gas phase, respectively.

## Results and discussion

### Choosing functionalization method

Figure 2 shows the results of $CO_2$ equilibrium adsorption on the functionalized adsorbents. In order to compare the influence of functionalization on adsorption capacity, adsorption isotherms were obtained at the temperature of 303.2 K and pressure up to 1 bar for pure $CO_2$ on COOH-amine-MWCNT, OH-amine-MWCNT and amine-MWCNT. The results indicate that amine-MWCNT possesses the highest adsorption capacity of $CO_2$. Because the results revealed that adding water in synthesis stage, which tended to produce amine-MWCNT, increased $CO_2$ adsorption capacity, further characterization COOH-amine-MWCNT, OH-amine-MWCNT were omitted from further characterization.

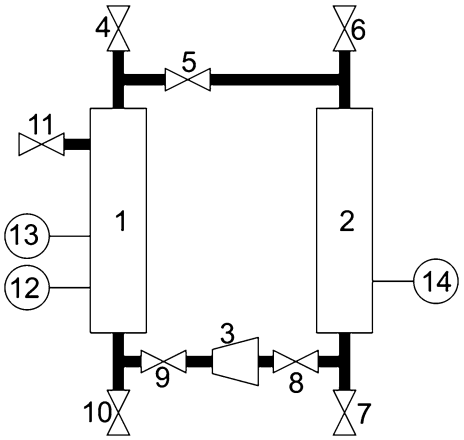


**Fig. 1** Schematic diagram of closed-loop volumetric apparatus (*1* loading cell, *2* adsorption cell, *3* circulating pump, *4–10* ball valve, *11* needle valve, *12* RH and temperature sensor, *13* pressure transmitter, *14* RTD temperature sensor)

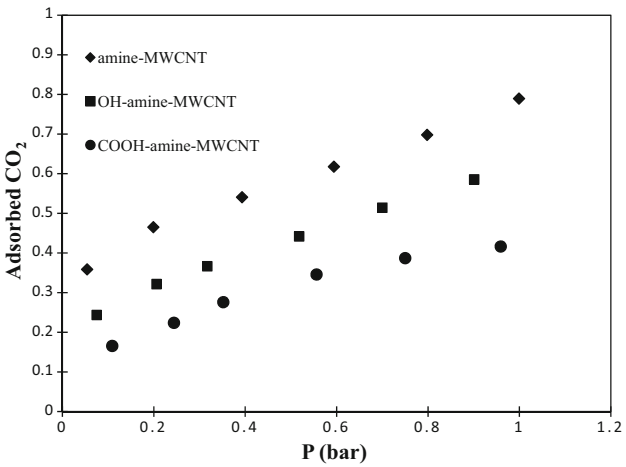


**Fig. 2** $CO_2$ adsorption on three different amine-functionalized MWCNTs at 303.2 K

## MWCNTs characterization

### *XRD*

XRD spectra of pristine MWCNT, OH-MWCNT and amine-MWCNT are shown in Fig. 3. As it is obvious, the general trends of all three plots, which can be ascribed to their crystalline arrangements, are very similar. Thus, it can be concluded that functionalization process did not affect graphitic structure of pristine MWCNTs. Obviously, these plots show the expectable characteristic of a MWCNT structure (Chen et al. 2009; Yu et al. 2012). The C(002) peak around $2\theta = 26.2°$ is flatten due to the limited number of layers and tube curvature. The expanded C(100) peak shows curved sheet of MWCNT (Chen et al. 2008). As shown in these patterns, intensity of C(002) in amine-MWCNT is much lower than OH-MWCNT. This can be attributed to the lower packing density in amine-MWCNT and also some defects caused by functionalization.

### *FTIR*

The FTIR spectra of adsorbents are shown in Fig. 4. The FTIR spectra of OH-MWCNT (Fig. 4a) and amine-MWCNT (Fig. 4b) possess a peak at 1571.7 and 1576.52 $cm^{-1}$, respectively, which is due to C=C double bond of nanotubes (Fatemi et al. 2011). Two peaks at 3421 and 1714 $cm^{-1}$ in spectrum of OH-MWCNT are attributed to hydroxyl (–OH) stretching vibration (Niu et al. 2007; Vuković et al. 2009) and C=O bonds (Fatemi et al. 2011), respectively. Simultaneous presence of these two peaks characterizes appearance of carboxyl group on the surface of OH-MWCNT (Fatemi et al. 2011; Vuković et al. 2010).

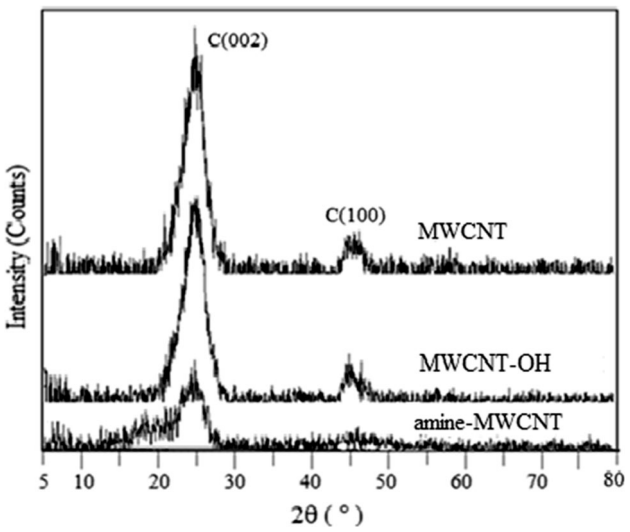


**Fig. 3** XRD patterns of MWCNT, OH-MWCNT and amine-MWCNT

Amine-MWCNT displays a peak at 3429.78 $cm^{-1}$, which is due to the $NH_2$ stretch of the amine group overlapped with hydroxyl stretching vibration (Vuković et al. 2009). Also, appearance of peaks at 2922.59 and 2855.1 $cm^{-1}$ after amine functionalization is ascribed to asymmetric and symmetric stretching vibrations of $CH_2$ groups, respectively (Vuković et al. 2010). Also, amine-MWCNT has peaks at 1654.62, 1186.97 and 1026.91 $cm^{-1}$ which can be attributed to N–H vibrations (Su et al. 2009), C-N bond stretching (Vuković et al. 2009) and Si–O–Si(C) vibrations (Su et al. 2009).

The appearance of C–$H_2$, N–$H_2$, N–H and Si–O–Si bonds after amine functionalization of MWCNT samples supports that TRI has been covalently attached on the surface of CNTs (Su et al. 2009). These functional groups serve as adsorption sites on the surface MWCNTs and increased adsorption capacity (Su et al. 2009; Vuković et al. 2010).

### *CHNS*

The results of elemental analysis of OH-MWCNT and amine-MWCNT indicated the formation of amine groups on the surface of amine-functionalized MWCNT. As shown in Table 2, hydrogen and nitrogen mass percentages of amine-MWCNT increased to 11.5 and 199 times as big as those of pristine MWCNT, respectively. This table can be also used to calculate the amount of intercalated amine groups in adsorbent. Since there exists 3 mol of nitrogen per each mol of TRI, the ratio of 7.98/(14 × 3) which is equal to $1.895 \times 10^{-3}$ mol per gram of adsorbent, will be obtained. By multiplying $1.895 \times 10^{-3}$ in molecular weight of TRI, the mass fraction of TRI in functionalized adsorbent is obtained about 31.64 %.

### *TGA*

These results will be used to find the onset of instability temperature and the weight loss present versus temperature of the studied samples. The weight loss percent data are employed to quantitative determination of functional groups on the surface of adsorbents.

Figure 5 shows TGA plots of pristine MWCNT, OH-MWCNT and amine-MWCNT. Due to existence of various functional groups on the surface of carbon nanotubes, their thermal decomposition involves several steps (Vuković et al. 2010). The first 1 % weight loss under 100 °C for all the samples is attributed to the adsorbed water vapor (Datsyuk et al. 2008; Su et al. 2009). Since the pristine MWCNT sample is used as received, the residual organic compounds during synthesis are removed from 350 to 500 °C. According to Fig. 5, this weight loss is about 2 %. The weight loss from 500 to 800 °C is associated with

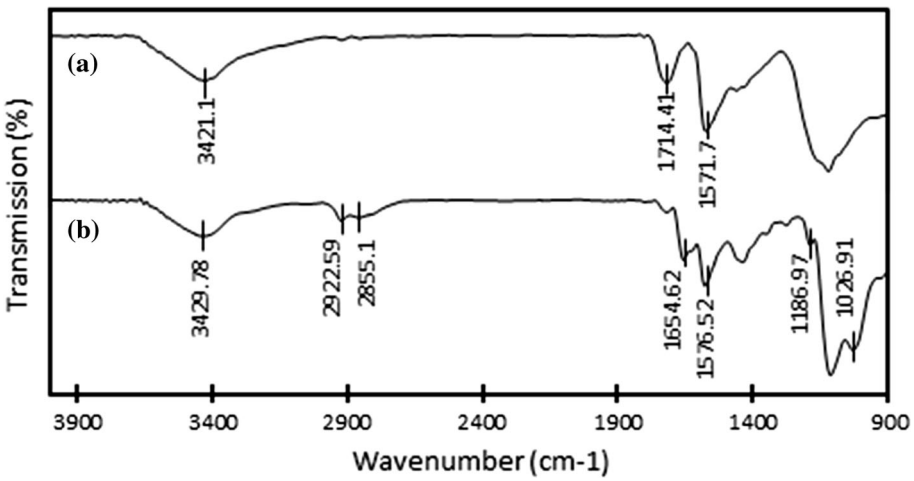


**Fig. 4** FTIR spectra of (*a*) OH-MWCNT and (*b*) amine-MWCNT

**Table 2** Elemental analysis of OH-MWCNT and amine-MWCNT

| Element mass percent | OH-MWCNT | Amine-MWCNT |
|---|---|---|
| Carbon | 91.47 | 66.49 |
| Nitrogen | 0.04 | 7.96 |
| Hydrogen | 0.35 | 4.03 |
| Sulfur | – | – |

oxidation of amorphous carbons present in the sample. After 800 °C, the weight of carbon nanotube declined steeply due to decomposing carbon nanotube structure. In the case of OH-MWCNT, about 2 % weight loss occurs at the temperature ranging from 170 to 350 °C that is ascribed to the removal of carboxyl functional groups present on the surface of OH-MWCNT. Further 3 % weight loss happening at the temperature range of 350 to 700 °C corresponds to the removal of hydroxyl functional groups present in the sample (Datsyuk et al. 2008). At a temperature higher than 700 °C, carbon nanotube structure is destroyed. For amine-MWCNT, approximately 30 % weight loss between 150 and 700 °C is occurred and related to the removal of the amine groups present on the surface of modified carbon nanotubes.

This result confirms the existence of about 30 wt% TRI on the surface of modified MWCNTs which is additionally proved by elemental analysis. The rapid weight loss after 700 °C is attributed to the decomposition of carbon nanotubes. TGA results show that MWCNT, OH-MWCNT and amine-MWCNT samples are thermally stable at the temperatures up to 350, 170 and 150 °C, respectively, and that these temperatures are more than regeneration temperatures of adsorbents.

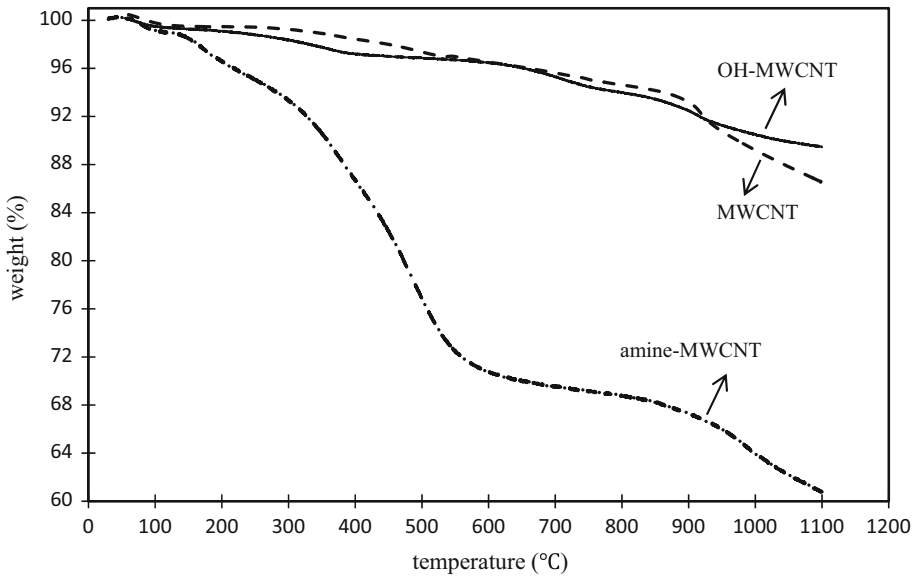


**Fig. 5** TGA results of MWCNT, OH-MWCNT and amine-MWCNT

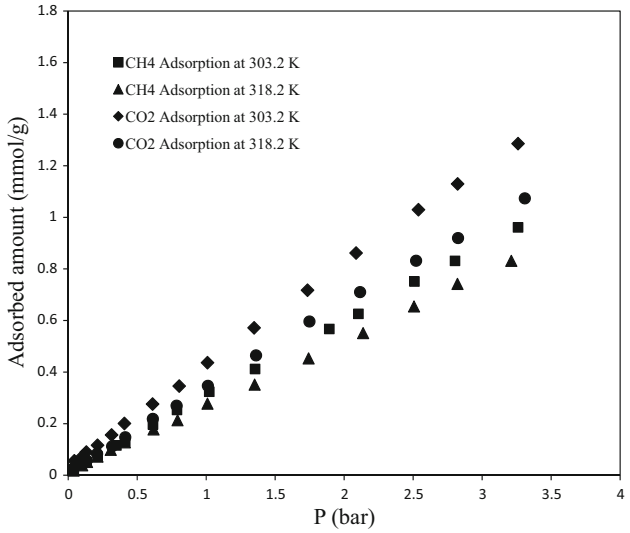


**Fig. 6** Adsorption isotherms of $CO_2$ and $CH_4$ on MWCNT at 303.2 and 318.2 K

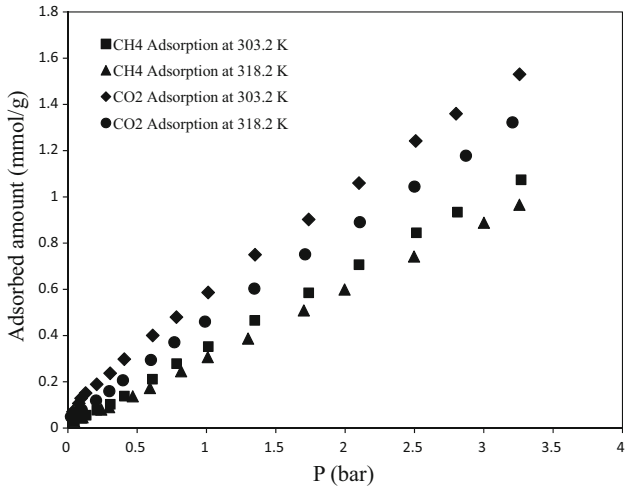


**Fig. 7** Adsorption isotherms of $CO_2$ and $CH_4$ on OH-MWCNT at 303.2 and 318.2 K

## Adsorption behaviors

### *Pure $CO_2$ and $CH_4$ adsorption*

Figures 6 through 8 show the adsorption isotherms at 303.2 and 318.2 K for pure $CO_2$ and $CH_4$ on pristine MWCNT, OH-MWCNT and amine-MWCNT, respectively. According to these figures, for both gases, adsorption capacity decreases as temperature rises, and the temperature dependency of carbon dioxide adsorption on amine-MWCNT is higher than those of the other two adsorbents. For all three adsorbents in whole ranges of temperature and pressure, adsorption capacity of carbon dioxide is higher

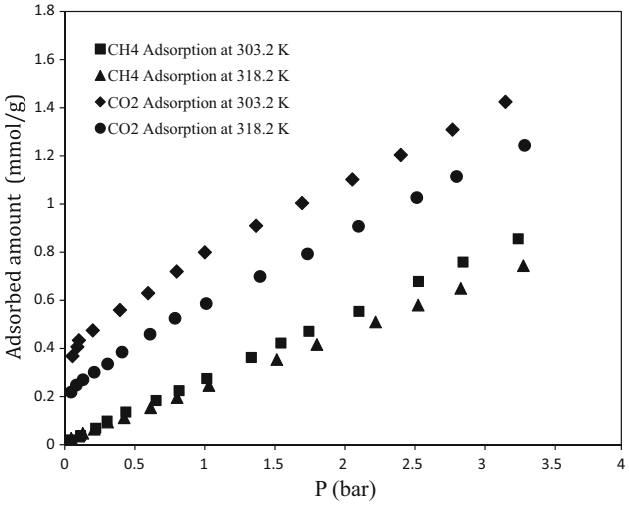


**Fig. 8** Adsorption isotherms of $CO_2$ and $CH_4$ on amine-MWCNT at 303.2 and 318.2 K

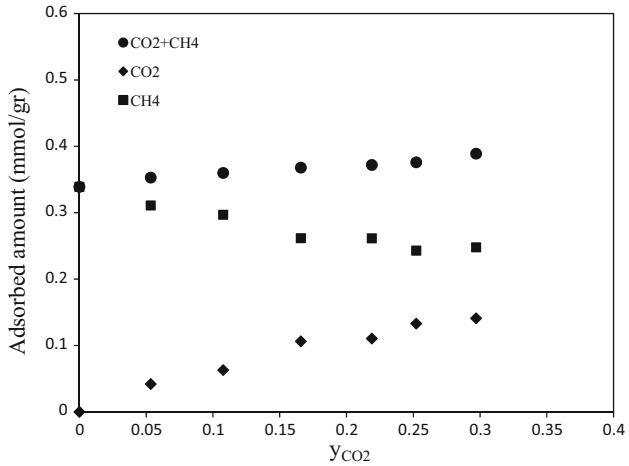


**Fig. 9** Equilibrium adsorption capacity for $CO_2$ and $CH_4$ in $CO_2$–$CH_4$ mixtures over MWCNT at 1 bar and 303.2 K

than methane. Also, the adsorption capacity of carbon dioxide is more sensitive to temperature than methane, in the whole ranges of pressure, probably due to stronger quadrupole interaction of $CO_2$ molecules with adsorption sites than nonpolar methane molecules.

According to Fig. 6, adsorption isotherms of methane and carbon dioxide on MWCNT are nearly linear. However, as shown in Figs. 7 and 8, adsorption isotherms of carbon dioxide for other adsorbents show a steep slope at lower pressures for $CO_2$, but not for methane. This gives evidence of a stronger interaction between carbon dioxide and amine or hydroxyl groups compared to methane. The adsorption behavior of three studied adsorbents can be summarized as follows for $CO_2$. At low pressures, amine-MWCNT demonstrates better performance in $CO_2$

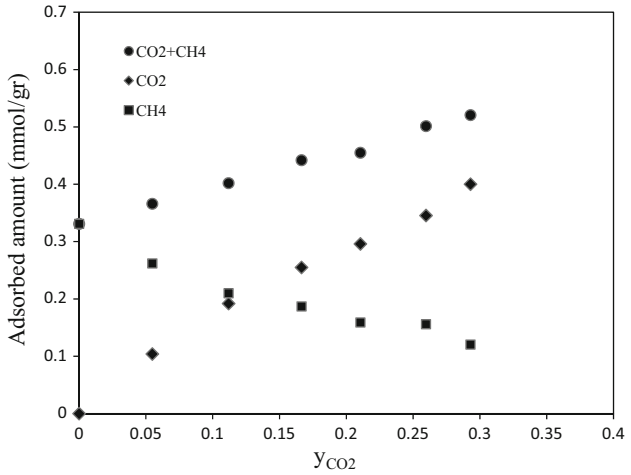


**Fig. 10** Equilibrium adsorption capacity for $CO_2$ and $CH_4$ in $CO_2$–$CH_4$ mixtures over amine-MWCNT at 1 bar and 303.2 K

**Table 3** $CO_2$ versus $CH_4$ adsorption selectivity as a function of the equilibrium molar fraction of $CO_2$ at 1 bar and 303.2 K

| MWCNT | | Amine-MWCNT | |
|---|---|---|---|
| $y_{CO_2}$ | Selectivity ($CO_2$/$CH_4$) | $y_{CO_2}$ | Selectivity ($CO_2$/$CH_4$) |
| 0.0534 | 2.39 | 0.0548 | 7.25 |
| 0.1077 | 1.76 | 0.1119 | 6.98 |
| 0.1658 | 2.04 | 0.1664 | 6.84 |
| 0.2189 | 1.51 | 0.2105 | 6.82 |
| 0.2522 | 1.62 | 0.2596 | 6.81 |
| 0.2970 | 1.34 | 0.2929 | 6.76 |

adsorption than the other two adsorbents do. Amine-MWCNT adsorbs nearly 2.5 and 4 times as much $CO_2$ as OH-MWCNT and pristine MWCNT at 303.2 K and 0.2 bar, respectively. The same conclusion for methane can also be presented as follows. Methane adsorption isotherms for the three adsorbents overlay at low pressure. This means that functional groups lose their abilities to adsorb methane at lower pressures. It can be attributed to the two facts, i.e., weak interaction of nonpolar methane molecules with both active sites of hydroxyl and amine groups at lower pressures and larger kinetic diameter of methane than $CO_2$. The latter hinders methane to penetrate into pores. At moderate to high pressures, adsorption capacity of OH-MWCNT is higher than those of other two adsorbents. It may be explained by two facts. First, internal pore volume in amine-MWCNT is decreased due to occupation by amine groups. Second, methane–hydroxyl group interaction is accelerated at higher pressures and it will be more influencing for less polar functional groups such as hydroxyl compared to amine group.

*Simultaneous adsorption of $CO_2$–$CH_4$*

Figures 9 and 10 show the equilibrium adsorption capacity of $CH_4$ and $CO_2$ from their binary mixture at 1 bar and 303.2 K for MWCNT and amine-MWCNT, respectively. Adsorption amounts of components have been calculated by using gas chromatograph (GC). According to experimental data, amine-MWCNT has higher $CO_2$/$CH_4$ selectivity than pristine MWCNT, an evidence of stronger quadrupole interaction of $CO_2$ molecules with adsorption sites than methane molecules. Thus, it can be concluded that functionalization of MWCNT with amine groups produces active sites on the surface of MWCNT and improves adsorption capacity and selectivity of $CO_2$ versus $CH_4$. Using data supplied by Figs. 9 and 10 and Eq. 1, $CO_2$/$CH_4$ selectivity as a function of the equilibrium molar fraction of $CO_2$ at 1 bar and 303.2 K was calculated and the results are shown in Table 3. As seen, $CO_2$/$CH_4$ selectivity for amine-MWCNT in all molar fractions of $CO_2$ is about 7, while for MWCNT is equal to average amount of 1.77. Although $CH_4$ molar fraction was dominant, the $CO_2$/$CH_4$ selectivity was higher than 1 in the whole range of molar fractions studied, especially for amine-MWCNT indicating that this adsorbent could be a promising material for separation of $CO_2$ from the mixture of $CO_2$-$CH_4$.

**Table 4** Adsorption parameters of Freundlich (Eq. 2) and Langmuir (Eq. 3) isotherms for $CO_2$ adsorption onto MWCNT, OH-MWCNT and amine-MWCNT

| Models | Parameters | MWCNT | | OH-MWCNT | | Amine-MWCNT | |
|---|---|---|---|---|---|---|---|
| | | 318.15 K | 303.15 K | 318.15 K | 303.15 K | 318.15 K | 303.15 K |
| Freundlich | $k_F$ (mmol/g)/(bar$^{1/n}$) | 0.44405 | 0.3476 | 0.597 | 0.468 | 0.853 | 0.631 |
| | $n$ | 1.104 | 1.06 | 1.266 | 1.137 | 2.5920 | 1.913 |
| | $R^2$ | 0.999 | 0.9997 | 0.9985 | 0.9991 | 0.9693 | 0.9788 |
| Langmuir | $q_m$ (mmol/gr) | 10.722 | 8.607 | 6.813 | 4.558 | 1.6595 | 1.466 |
| | $b$ (1/bar) | 0.0535 | 0.0334 | 0.1502 | 0.0733 | 1.686 | 0.6499 |
| | $R^2$ | 0.9982 | 0.9997 | 0.9937 | 0.9978 | 0.9541 | 0.970 |

**Table 5** Adsorption parameters of Freundlich (Eq. 2) and Langmuir (Eq. 3) isotherms for $CH_4$ adsorption onto MWCNT, OH-MWCNT and amine-MWCNT

| Models | Parameters | MWCNT | | OH-MWCNT | | Amine-MWCNT | |
|---|---|---|---|---|---|---|---|
| | | 318.15 K | 303.15 K | 318.15 K | 303.15 K | 318.15 K | 303.15 K |
| Freundlich | $k_F$ (mmol/g)/(bar$^{1/n}$) | 0.3130 | 0.2739 | 0.3471 | 0.3015 | 0.2785 | 0.2455 |
| | $n$ | 1.056 | 1.055 | 1.044 | 1.015 | 1.076 | 1.047 |
| | $R^2$ | 0.9996 | 0.999 | 0.9996 | 0.9995 | 0.9995 | 0.999 |
| Langmuir | $q_m$ (mmol/gr) | 11.418 | 11.135 | 25.319 | 13.514 | 12.092 | 7.396 |
| | $b$ (1/bar) | 0.0287 | 0.0243 | 0.0263 | 0.0121 | 0.0338 | 0.0234 |
| | $R^2$ | 0.9994 | 0.9984 | 0.9996 | 0.9995 | 0.9992 | 0.9982 |

*Correlating experimental data of pure gases by Freundlich and Langmuir isotherms*

The parameters of Freundlich and Langmuir isotherms were obtained by fitting to the obtained experimental data. The Freundlich and Langmuir model is expressed by Eqs. 2 and 3, respectively:

$$q = k_F(P)^{1/n} \quad (2)$$

$$q = q_m\, bP/(1 + bP) \quad (3)$$

where the parameters of these models are reported in Tables 4 and 5. According to Tables 4 and 5, parameter $n$ in Freundlich model for methane adsorption is approximately unity for all adsorbents; however, in the case of $CO_2$ adsorption on OH-MWCNT and amine-MWCNT this parameter strongly deviates from unity. It means that there exists a significant nonlinear dependency of the adsorption capacity on pressure for $CO_2$ in comparison with methane. Parameter $b$ in Langmuir model for methane adsorption on the three different adsorbents is much lower than those for $CO_2$. It indicates a weak interaction between methane and adsorption sites. This observation is consistent with our experimental data and can be interpreted with the behavior of carbon dioxide as a strong quadrupole and methane as a nonpolar molecule. Langmuir model shows better agreement with the experimental data of MWCNT and OH-MWCNT than those of amine-MWCNT for $CO_2$ adsorption. It means that the distribution of adsorption sites on amine-MWCNT is more heterogeneous than two other adsorbents.

## Conclusion

OH-MWCNT and COOH-MWCNT were functionalized by TRI, and the effect of existence of water during process was investigated. Results showed the superior performance of functionalized OH-MWCNT in the presence of water than other functionalized samples. The adsorption equilibrium isotherms of $CO_2$ and $CH_4$ on pristine MWCNT, OH-MWCNT and amine-MWCNT were obtained at 303.2 and 318.2 K. At low pressures, the $CO_2$ adsorption performance of amine-MWCNT is better than those of the other two sorbents. It was found that adsorption capacity of $CO_2$ on three types of MWCNT follows the order of amine-MWCNT > OH-MWCNT > MWCNT at both 303.2 K and 318.2 K.

At gage pressure lower than 1 bar and temperature of 303.2 K, adsorption capacity of carbon dioxide on MWCNT, OH-MWCNT and amine-MWCNT was 0.436 and 0.586 and 0.8 mmol per gram of adsorbent, respectively. In the case of $CH_4$, these values, respectively, were 0.323, 0.352 and 0.275. Simultaneous adsorption of $CO_2$ and $CH_4$ results showed $CO_2/CH_4$ selectivity for MWCNT and amine-MWCNT in all molar fractions of $CO_2$ is about 1.77 and 7, respectively, indicating that amine-MWCNT could be a promising material for separation of $CO_2$ from the mixture of $CO_2$–$CH_4$. Experimental data of pure gases were well correlated by Freundlich and Langmuir equations.

**Acknowledgment** We would like to thank financial support from Department of Research Affair of University of Isfahan and Central Laboratory of University of Isfahan.

## References

Balasubramanian K, Burghard M (2005) Chemically functionalized carbon nanotubes. Small 1(2):180–192

Chen L, Xie H, Li Y, Yu W (2008) Surface chemical modification of multiwalled carbon nanotubes by a wet-mechanochemical reaction. J Nanomater 63:1–5

Chen C, Hu J, Shao D, Li J, Wang X (2009) Adsorption behavior of multiwall carbon nanotube/iron oxide magnetic composites for Ni (II) and Sr (II). J Hazard Mater 164(2):923–928

Chiang YC, Wu PY (2010) Adsorption equilibrium of sulfur hexafluoride on multi-walled carbon nanotubes. J Hazard Mater 178(1):729–738

Chiang YC, Lin WH, Chang YC (2012) The influence of treatment duration on multi-walled carbon nanotubes functionalized by $H_2SO_4/HNO_3$ oxidation. Appl Surf Sci 257(6):2401–2410

Dai XD, Liu XM, Zhao G, Qian L, Qiao K, Yan ZF (2008) Treatment of activated carbon for methane storage. Asia-Pacific J Chem Eng 3(3):292–297

Datsyuk V, Kalyva M, Papagelis K, Parthenios J, Tasis D, Siokou A et al (2008) Chemical oxidation of multiwalled carbon nanotubes. Carbon 46(6):833–840

Deng H, Yi H, Tang X, Yu Q, Ning P, Yang L (2012) Adsorption equilibrium for sulfur dioxide, nitric oxide, carbon dioxide, nitrogen on 13X and 5A zeolites. Chem Eng J 188:77–85

Fatemi S, Vesali-Naseh M, Cyrus M, Hashemi J (2011) Improving $CO_2/CH_4$ adsorptive selectivity of carbon nanotubes by functionalization with nitrogen-containing groups. Chem Eng Res Des 89(9):1669–1675

Gholami M, Talaie MR, Aghamiri SF (2014) Direct synthesis of bimodal porous structure MCM-41 and its application in $CO_2$ capturing through amine-grafting. Korean J Chem Eng 31(2):322–326

Harlick PJ, Sayari A (2007) Applications of pore-expanded mesoporous silica. 5. Triamine grafted material with exceptional $CO_2$ dynamic and equilibrium adsorption performance. Ind Eng Chem Res 46(2):446–458

Hsu SC, Lu C, Su F, Zeng W, Chen W (2010) Thermodynamics and regeneration studies of $CO_2$ adsorption on multiwalled carbon nanotubes. Chem Eng Sci 65(4):1354–1361

Huang L, Zhang L, Shao Q, Lu L, Lu X, Jiang S, Shen W (2007) Simulations of binary mixture adsorption of carbon dioxide and methane in carbon nanotubes: temperature, pressure, and pore size effects. J Phys Chem C 111:11912–11920

Ju S, Lee JM, Jung Y, Lee E, Lee W, Kim SJ (2010) Highly sensitive hydrogen gas sensors using single-walled carbon nanotubes grafted with Pd nanoparticles. Sens Actuators B Chem 146(1):122–128

Kuzmany H, Kukovecz A, Simon F, Holzweber M, Kramberger C, Pichler T (2004) Functionalization of carbon nanotubes. Synth Met 141(1):113–122

Labus K, Gryglewicz S, Machnikowski J (2014) Granular KOH-activated carbons from coal-based cokes and their $CO_2$ adsorption capacity. Fuel 118:9–15

Lithoxoos GP, Labropoulos A, Peristeras LD, Kanellopoulos N, Samios J, Economou IG (2010) Adsorption of $N_2$, $CH_4$, CO and $CO_2$ gases in single walled carbon nanotubes: a combined experimental and Monte Carlo molecular simulation study. J Supercrit Fluids 55(2):510–523

Mahdavifar Z, Haghbayan M (2012) Theoretical investigation of pristine and functionalized AlN and SiC single walled nanotubes as an adsorption candidate for methane. Appl Surf Sci 263:553–562

Nickmand Z, Aghamiri SF, Khozanie MRT, Sabzyan H (2013) A Monte Carlo simulation of the adsorption of $CO_2$ and $SO_2$ gases in pure and functionalized single walled carbon nanotubes. Sep Sci Technol. doi:10.1080/01496395.2013.862277

Niu L, Luo Y, Li Z (2007) A highly selective chemical gas sensor based on functionalization of multi-walled carbon nanotubes with poly (ethylene glycol). Sens Actuators B Chem 126(2):361–367

Oriňáková R, Oriňák A (2011) Recent applications of carbon nanotubes in hydrogen production and storage. Fuel 90(11):3123–3140

Ottiger S, Pini R, Storti G, Mazzotti M (2008) Competitive adsorption equilibria of $CO_2$ and $CH_4$ on a dry coal. Adsorption 14(4–5):539–556

Pham TD, Xiong R, Sandler SI, Lobo RF (2014) Experimental and computational studies on the adsorption of $CO_2$ and $N_2$ on pure silica zeolites. Microporous Mesoporous Mater 185:157–166

Plaza M, Pevida C, Arenillas A, Rubiera F, Pis J (2007) $CO_2$ capture by adsorption with nitrogen enriched carbons. Fuel 86(14):2204–2212

Saha D, Bao Z, Jia F, Deng S (2010) Adsorption of $CO_2$, $CH_4$, $N_2O$, and $N_2$ on MOF-5, MOF-177, and zeolite 5A. Environ Sci Technol 44:1820–1826

Sayari A, Belmabkhout Y, Serna-Guerrero R (2011) Flue gas treatment via $CO_2$ adsorption. Chem Eng J 171(3):760–774

Silva JAC, Cunha AF, Schumann K, Rodrigues AE (2014) Binary adsorption of $CO_2/CH_4$ in binderless beads of 13X zeolite. Microporous Mesoporous Mater 187:100–107

Sinnott SB (2002) Chemical functionalization of carbon nanotubes. J Nanosci Nanotechnol 2(2):113–123

Su F, Lu C, Cnen W, Bai H, Hwang JF (2009) Capture of $CO_2$ from flue gas via multiwalled carbon nanotubes. Sci Total Environ 407(8):3017–3023

Tagliabue M, Rizzo C, Millini R, Dietzel PD, Blom R, Zanardi S (2011) Methane storage on CPO-27-Ni pellets. J Porous Mater 18(3):289–296

Trykowski G, Biniak S, Stobinski L, Lesiak B (2010) Preliminary investigations into the purification and functionalization of multiwall carbon nanotubes. Acta Phys Pol Ser A Gen Phys 118(3):515

Vela S, Huarte-Larrañaga F (2011) A molecular dynamics simulation of methane adsorption in single walled carbon nanotube bundles. Carbon 49(13):4544–4553

Vuković G, Marinković A, Obradović M, Radmilović V, Čolić M, Aleksić R et al (2009) Synthesis, characterization and cytotoxicity of surface amino-functionalized water-dispersible multiwalled carbon nanotubes. Appl Surf Sci 255(18):8067–8075

Vuković GD, Marinković AD, Čolić M, Ristić MĐ, Aleksić R, Perić-Grujić AA et al (2010) Removal of cadmium from aqueous solutions by oxidized and ethylenediamine-functionalized multiwalled carbon nanotubes. Chem Eng J 157(1):238–248

Wiśniewski M, Furmaniak S, Kowalczyk P, Werengowska KM, Rychlicki G (2012) Thermodynamics of benzene adsorption on oxidized carbon nanotubes—experimental and simulation studies. Chem Phys Lett 538:93–98

Xiao P, Zhang J, Webley P, Li G, Singh R, Todd R (2008) Capture of $CO_2$ from flue gas streams with zeolite 13X by vacuum-pressure swing adsorption. Adsorption 14(4–5):575–582

Xu Yj, Rosa A, Liu X, Su DS (2011) Characterization and use of functionalized carbon nanotubes for the adsorption of heavy metal anions. New Carbon Mater 26(1):57–62

Yu F, Ma J, Wu Y (2012) Adsorption of toluene, ethylbenzene and xylene isomers on multi-walled carbon nanotubes oxidized by different concentration of NaOCl. Front Environ Sci Eng 6(3):320–329

Zamora B, Roque J, Balmaseda J, Reguera E (2010) Methane storage in prussian blue analogues and related porous solids: nature of the involved adsorption forces. Z Anorg Allg Chem 636(15):2574–2578

Zhang X, Shao X, Wang W, Cao D (2010a) Molecular modeling of selectivity of single-walled carbon nanotube and MCM-41 for separation of methane and carbon dioxide. Sep Purif Technol 74(3):280–287

Zhang Z, Xu M, Wang H, Li Z (2010b) Enhancement of $CO_2$ adsorption on high surface area activated carbon modified by $N_2$, $H_2$ and ammonia. Chem Eng J 160(2):571–577

Zhang J, Clennell MB, Dewhurst DN, Liu K (2014) Combined Monte Carlo and molecular dynamics simulation of methane adsorption on dry and moist coal. Fuel 122:186–197

Zhao G, Aziz B, Hedin N (2010) Carbon dioxide adsorption on mesoporous silica surfaces containing amine-like motifs. Appl Energy 87(9):2907–2913